TN 58-226
ASTIA AD 154-128

ENGINEERING RESEARCH INSTITUTE
THE UNIVERSITY OF MICHIGAN
ANN ARBOR

Technical Note

DESCRIPTION AND EXPERIMENTAL RESULTS OF TWO REGENERATIVE HEAT EXCHANGERS

E. K. Dabora
M. P. Moyle
R. Phillips
J. A. Nicholls
P. L. Jackson

Aircraft Propulsion Laboratory
Department of Aeronautical Engineering

ERI Project 2284

COMBUSTION DYNAMICS DIVISION
AIR FORCE OFFICE OF SCIENTIFIC RESEARCH
AIR RESEARCH AND DEVELOPMENT COMMAND
CONTRACT NO. AF 18(600)-1199
WASHINGTON, D. C.

February 1958

EXCN
UMR 0742

ACKNOWLEDGMENT

This report is part of the research program which is supported by the United States Air Force through the Air Force Office of Scientific Research of the Air Research and Development Command, under Contract No. AF 18(600)-1199. The assistance of this agency is gratefully acknowledged.

TABLE OF CONTENTS

LIST OF FIGURES

NOMENCLATURE

a	=	Viscous resistance coefficient, ft^{-2}
b	=	Inertial resistance coefficient, ft^{-1}
C	=	Heat capacity of heat-exchanger bed material per unit volume, $Btu/ft^3\text{-}°F$
c_p	=	Specific heat of fluid at constant pressure, Btu/lbm°F
G	=	Mass rate of flow per unit area, $lbm/ft^2\text{-}sec$
h	=	Heat-transfer coefficient between fluid and bed material, $Btu/sec - ft^{2}°F$
$I_o()$	=	Modified Bessel function of the first kind and zero order
ℓ	=	b/a = characteristic length, ft
ΔP	=	Pressure drop, lbf/ft^2
Pr	=	$c_p\mu/k$ = Prandtl number
Re	=	$\ell G/\mu$ = Reynolds number
s	=	Heat-transfer surface area of bed material/unit volume of bed material, ft^2/ft^3
s_o	=	Heat-loss surface area of exchanger/unit volume of bed material, ft^2/ft^3
St	=	$sh\ell/Gc_p$ = Stanton number
T	=	Fluid temperature, °F
T_i	=	Fluid inlet temperature, °F
t	=	Bed-material temperature, °F
t_o	=	Bed-material temperature at zero time, °F
t_s	=	Temperature of surroundings, °F
U_o	=	Overall-heat-transfer coefficient to surroundings based on area s_o
V	=	Fluid velocity, ft/sec
w	=	Mass flow rate, lbm/sec
x	=	Heat-exchanger length, ft

Greek Letters

α	=	$s_o U_o/sh$ nondimensional heat-transfer ratio
δ	=	Nondimensional bed temperature
η	=	$sh\tau/C$ = reduced time
θ	=	Nondimensional fluid temperature
μ	=	Viscosity of fluid, lbm/ft - sec
ξ	=	shx/Gc_p reduced length of heat exchanger
ρ	=	Specific weight of fluid, lbm/ft^3
τ	=	Time, sec

Subscripts

ss	=	Steady-state
1,2	=	Refers to two different stations along heat exchanger

ABSTRACT

Two pebble-type regenerative heat exchangers capable of operating at pressures and temperatures beyond the limits of commercially available equipment have been designed and constructed by personnel of the Aircraft Propulsion Laboratory. These heat exchangers were required to produce stagnation temperatures of the order of 2500°R at pressures of the order of 1000 psi in experiments designed to achieve a standing detonation wave.

In the initial operation, the outlet temperature of the small(hydrogen) heat exchanger was considerably less than anticipated. As a result of this, a theory was developed to predict the performance of a regenerative heat exchanger with heat loss; this analysis was reported in Ref. 7. The design and operating characteristics of the two heat exchangers are presented in this report and their performance is compared with the analysis presented in Ref. 7. The experimental results agree very well with the theory.

The heat-transfer characteristics obtained during evaluation of the exchangers showed that heat-transfer coefficients were lower than values reported in the literature for the same type of bed material. Thus it is recommended that the latter values be used cautiously in any design.

OBJECTIVE

The object of this report is to describe two pebble-type regenerative heat exchangers built at the Aircraft Propulsion Laboratory and to present the experimental results obtained with them.

I. INTRODUCTION

In Ref. 1 it was shown that high pressures and high stagnation temperatures would be required in any experimental installation for studying a standing detonation wave. The pressures and temperatures theoretically required were reported to be beyond the limits of commercially available equipment. Since high-temperature, high-pressure gases are required in the simulation of flight stagnation conditions in the supersonic and hypersonic regions, a facility designed to achieve a standing detonation wave would be useful in other research in the field of high-speed aerodynamics. Therefore, the design and construction of a facility capable of flight simulation at high Mach numbers was undertaken by personnel at the Aircraft Propulsion Laboratory.

There are similar installations which have been designed and operated throughout the country, e.g., at the University of Minnesota,[2] Polytechnic Institute of Brooklyn,[3] University of Texas, and NACA Langley Field. Although these facilities are somewhat similar to the one described herein, it is believed there is enough dissimilarity (such as methods of heating, blowdown, and heat-loss characteristics, etc.) to warrant making the information available to future designers. This information includes experimental values of the heat-transfer coefficient obtained and comparison of them with those reported in the present literature.

II. DESCRIPTION OF THE HEAT EXCHANGERS

The heat exchangers described here for producing high-temperature air and hydrogen are of the regenerative type. Briefly, they operate as follows:

hot gases produced by the combustion of propane-air mixture are passed over a bed of refractory pebbles until the downstream end of the bed reaches the temperature required or slightly above it. Then the gas which is to be heated is passed through the heat exchanger from where it emerges at the desired temperature. Since the gases are compressed, there is an additional requirement for the heat exchangers: namely, they must withstand pressures in the neighborhood of 1000 psi. The air heat exchanger will be described in detail here but only a brief description of the hydrogen heat exchanger will be given.

Figure 1 shows the layout of the air heat exchanger. It consists of a 14-ft-long Navy Surplus Catapult steel cylinder, 24-in. OD by 18-in. ID (1), lined with lap-joined ceramic rings 12 in. long and 12.5-in. ID (2), and with ceramic retainer (3) and plug (8) at the end. Between the ceramic rings and the shell, ceramic grog is packed to allow for any differences in radial expansion. An allowance for longitudinal expansion is also made by making the total length of the liner shorter than the shell. The space inside the liner is filled with 3/8-in. alumina pebbles which make up the heat-storage medium. Figure 1 shows the upstream end of the heat exchanger with the burner attached.

The other end (downstream end) is similar but of course without the burner. The burner (7) is a stainless-steel cylinder with ceramic liner. A flame holder consisting of two 1/4-in. stainless-steel rods at right angle to each other is located at the inlet to the burner. Part (11) is the mixing chamber where propane and air are mixed before entering the burner. At the exit of the mixing chamber a provision for a spark plug is made to initiate combustion.

The design of the hydrogen heat exchanger is similar to that of the air heat exchanger except that the OD of the shell is 4.75 in., the OD of the

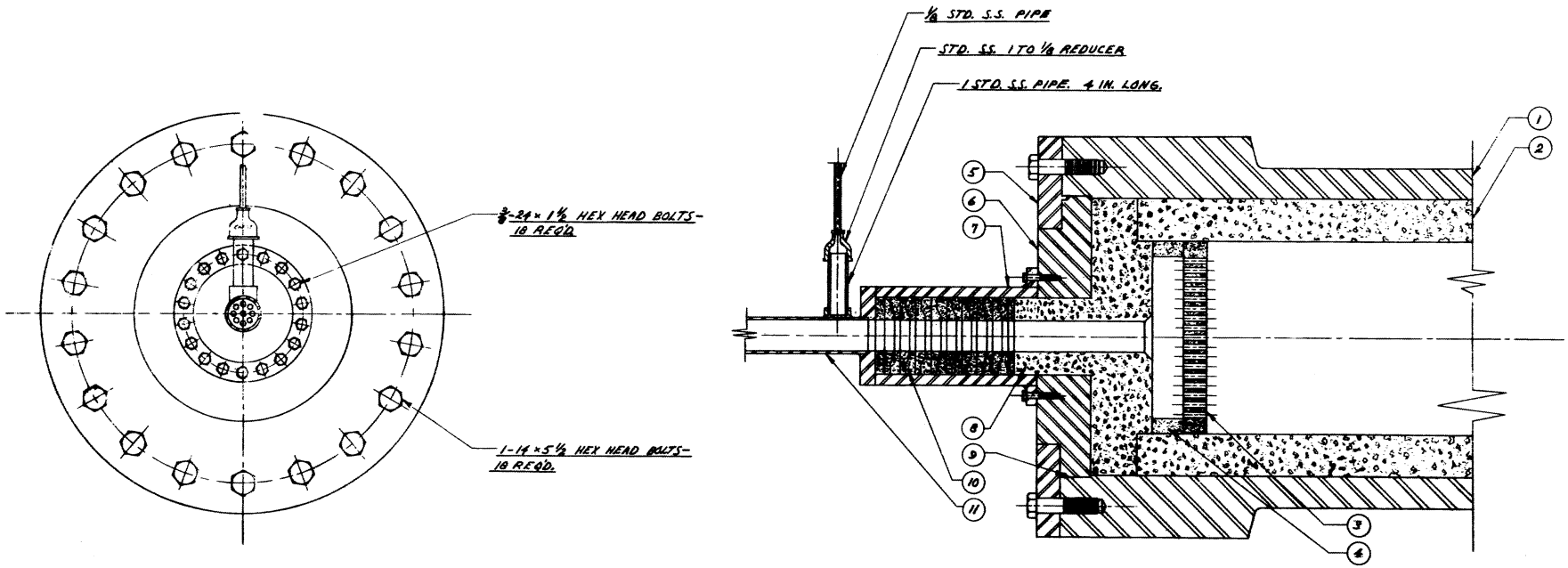

Fig. 1. Layout of air heat exchanger.

liner is 3.25 in. and its ID is 1.75 in.

Figure 2 shows the physical arrangement of the heat exchangers and the flow controls. A schematic diagram of the flow system is shown in Fig. 3. The operation of the system may be described as follows: the air and the hydrogen heat exchangers are heated by the products of combustion of propane air mixture, and then air and hydrogen are heated by passing them through the heat exchangers. The separately heated air and hydrogen are finally mixed together at the nozzle inlet. As shown in Fig. 2, the two heat exchangers are placed in a water bath to maintain low shell temperature. In actual operation this temperature never exceeded 180°F.

The flow rates are measured by thin-plate orifices designed according to ASME specifications and temperatures at the inlets and exits of the heat exchangers are made by Platinum-Platinum Rhodium thermocouples and recorded by a Consolidated Engineering Corp. oscillograph. In each heat exchanger, measurement of the wall temperature at three locations along the length is made by iron-constantan thermocouples.

III. EXPERIMENTAL RESULTS AND COMPARISON WITH THEORY

The regenerative-heat-exchanger theory is pretty well established for the adiabatic (no heat loss) type of exchanger.[4,5,6] The design of the two heat exchangers described above was made according to Ref. 6, with provision of insulation and an estimate of the heat loss. However, despite these precautions, the hydrogen heat exchanger proved to be inadequate because the exit temperature remained very low during the heating part of the cycle. This led to a closer investigation of the heat loss and a theoretical analysis was developed in Ref. 7 to include this loss.

According to Ref. 7, if the inlet temperature is constant and the heat-

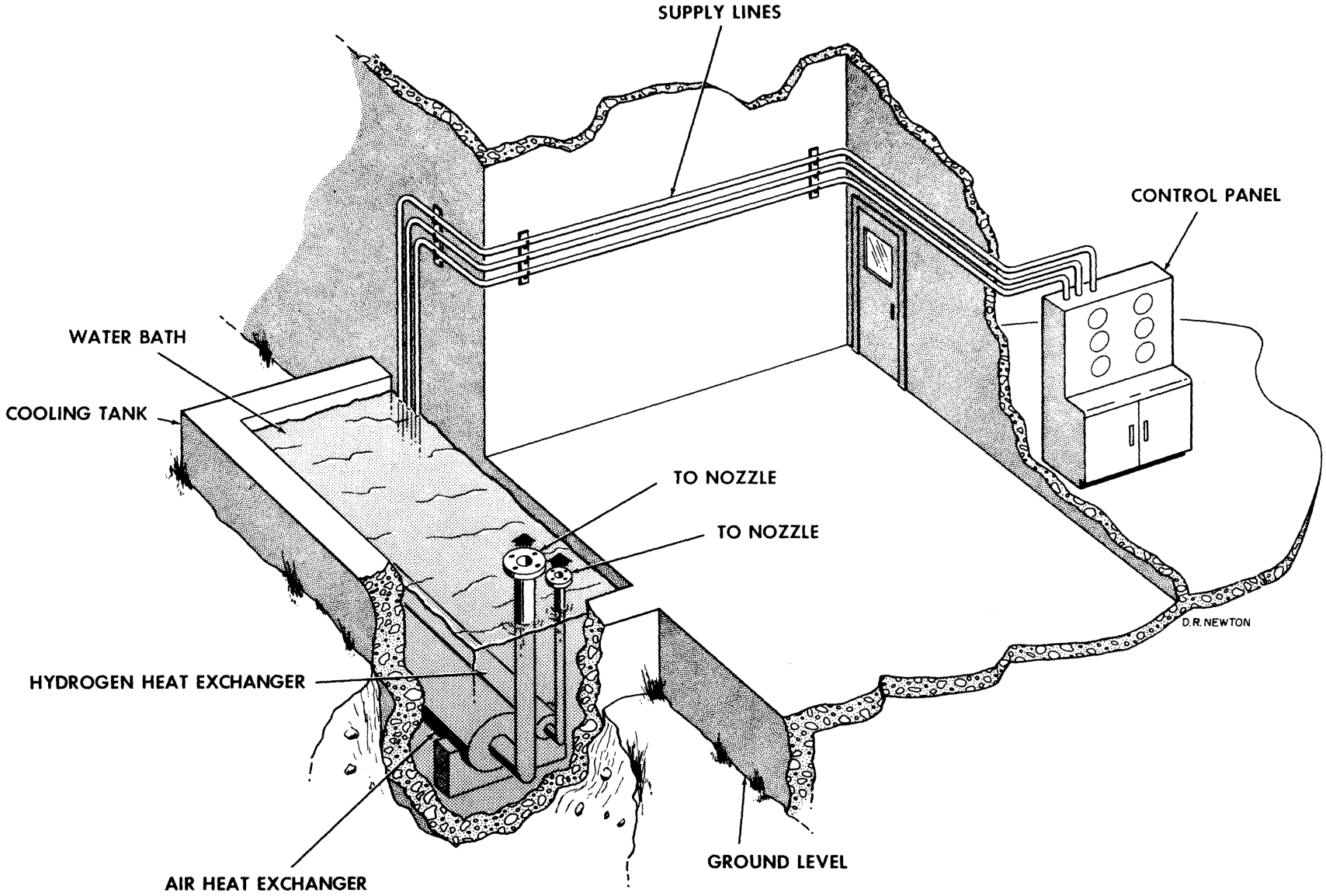

Fig. 2. Physical arrangement of the heat exchangers and controls.

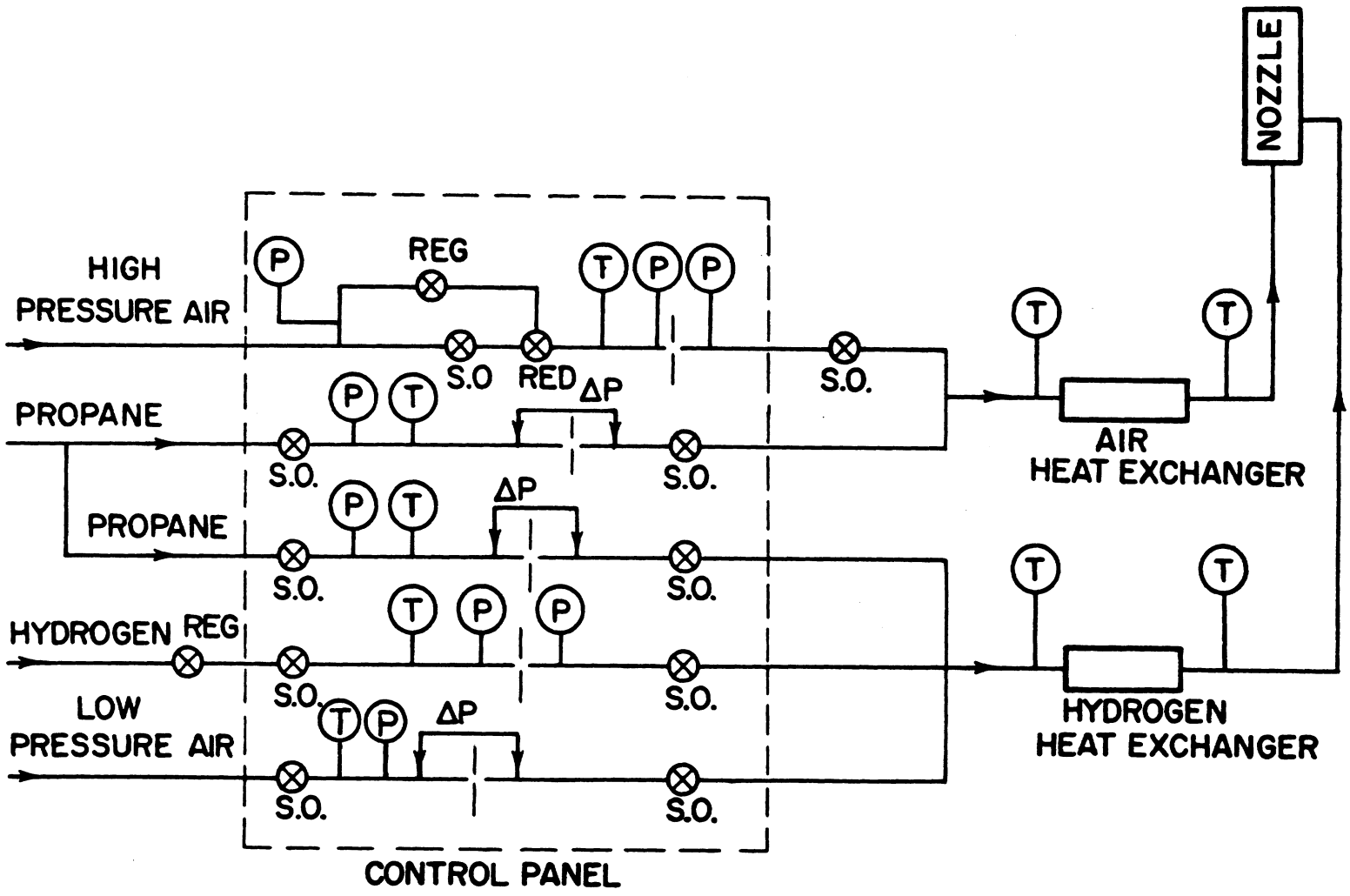

Fig. 3. Schematic diagram of flow system.

exchanger bed is at a uniform temperature lower than the inlet temperature of the gas at time zero, then the nondimensional form of the equations for the bed and gas temperatures as a function of time and length of heat exchanger is as follows:

$$\delta = e^{-\alpha\xi} \int_0^{\eta} e^{-(\eta+\xi)} I_0(2\sqrt{\xi\eta})\, d\eta \quad , \tag{1}$$

$$\theta = e^{-\alpha\xi} \left[e^{-(\eta+\xi)} I_0(2\sqrt{\xi\eta}) + \int_0^{\eta} e^{-(\eta+\xi)} I_0(2\sqrt{\xi\eta})\, d\eta \right] , \tag{2}$$

where:

$$\delta = \frac{t - t_o}{T_i - t_o} \quad ,$$

$$\theta = \frac{T - t_o}{T_i - t_o} \quad ,$$

$$\xi = \frac{shx}{Gc_p} \quad ,$$

$$\eta = \frac{sh\tau}{C} \quad , \text{ and}$$

$$\alpha = \frac{s_o U_o}{sh} \quad .$$

The above two expressions for bed and gas temperatures differ from the adiabatic heat-exchanger solutions by the factor $e^{-\alpha\xi}$ only. Thus, a plot of θ/θ_{ss} vs. η for various values of ξ will be the same as that of θ vs. η for the adiabatic case. Here θ_{ss} is the steady-state gas temperature, i.e.,

$$\theta_{ss} = e^{-\alpha\xi} \quad . \tag{3}$$

Such a plot, based on numerical tables in Ref. 8, is shown in Fig. 4 on a semi-log scale. The reasons for this choice of coordinates will become apparent later.

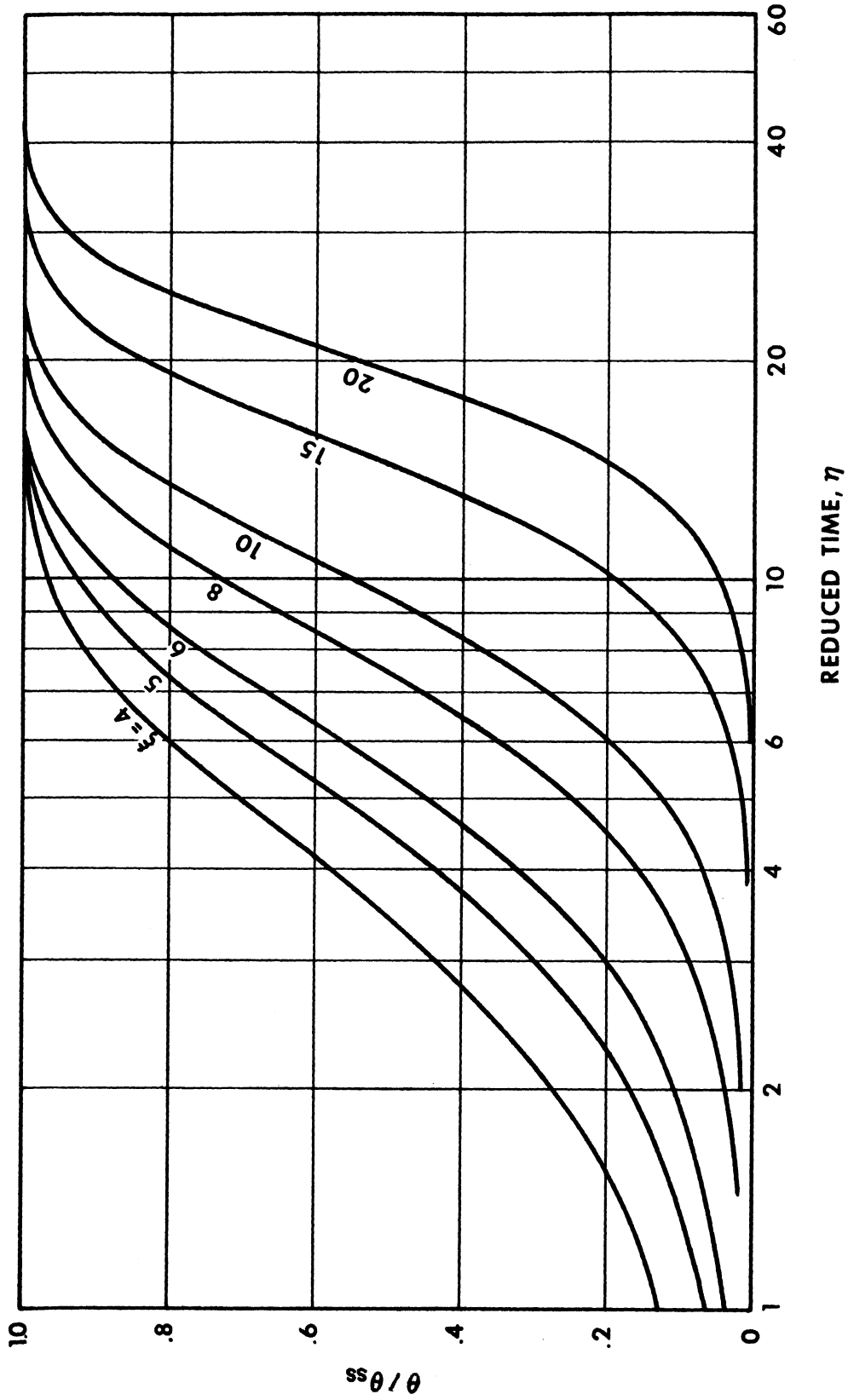

Fig. 4. θ/θ_{ss} vs. η at various values of ξ.

Because of the high inlet temperature of the gas, there was some doubt as to the accuracy of its measurement. However, a method of deducing this temperature is described here. If the steady-state temperature of the gas is made at two locations along the heat exchanger, then

$$\theta_{ss_1} = e^{-\alpha\xi_1} \quad , \tag{4}$$

$$\theta_{ss_2} = e^{-\alpha\xi_2} \quad . \tag{5}$$

Taking the logarithm of the ratio of (4) and (5), we get

$$\ell n \frac{\theta_{ss_1}}{\theta_{ss_2}} = (\xi_2 - \xi_1)\alpha \tag{6}$$

or

$$\ell n \frac{T_{ss_1} - t_o}{T_{ss_2} - t_o} = \frac{s_o U_o}{G c_p}(x_2 - x_1) \quad . \tag{7}$$

Since G, c_p, x_1, x_2, T_{ss_1}, T_{ss_2}, and t_o are known or measurable quantities, the product $s_o U_o$ can be evaluated. Now using either Eq. (4) or (5) the inlet temperature, T_{in} , can be determined since Eq. (4), for example, can be rewritten as:

$$\frac{T_{ss_1} - t_o}{T_{in} - t_o} = e^{-s_o U_o / G c_p} \quad . \tag{4a}$$

This is what has been done for the hydrogen heat exchanger and the result indicated very close agreement with the measured temperature.

To correlate the experimental data with the theoretical analysis, a knowledge of heat-transfer coefficient is necessary. Since heat-transfer data for randomly packed pellets are not very well established, it was decided to calculate the heat-transfer coefficient from the experimental results using essentialy the technique used in Ref. 6. This technique is based on the fact

that the shape of the curves of θ vs. η is unique for constant ξ. This can easily be confirmed from Fig. 4. Now from the data obtained, one can plot on semi-log paper $T-t_o/T_{ss}-t_o$ vs. time, τ. With the assumption that sh/C is constant, τ becomes proportional to η and on the log scale it will be different from η by a constant. Hence the plot should have the same shape as the corresponding theoretical curve. The plot is usually made on transparent paper and placed on the theoretical curves, such as Fig. 4, with the abscissas coinciding. Then the transparent paper is moved along the abscissa until the experimental points lie on one of the theoretical curves. Thus ξ is determined and since G, C_p, and x are known, one can find sh. In addition a correspondence between η and τ is found, and since sh is determined, C can also be determined. C in this case will be the apparent heat capacity per unit volume of the bed material which should be equal to the heat capacity of the bed material plus a pro-rated heat capacity of the insulation per unit volume of the bed material. This can be quite high. For example, in the case of the hydrogen heat exchanger the heat capacity of the bed material alone is 31 Btu/ft^3°F, whereas the apparent heat capacity turned out to be 110 Btu/ft^3°F.

The value of ξ as determined by the method just described was checked by another method. Locke in Ref. 9 has shown that the slope $[d\theta/d(\eta/\xi)]_{max}$ is a function of ξ alone for the adiabatic case. For the nonadiabatic case, the value of the slope is different by a factor of $e^{-\xi\alpha}$ only, which is independent of sh. The slope is also independent of sh; hence, by evaluating it graphically, one can determine ξ from which sh can be determined. The data reported herein were checked as described and found to agree very closely with those obtained by the original method. After having determined sh and C as described above, a plot of θ vs. η can be made. Since $e^{-\alpha\xi}$ can be determined from Eq. (3), the theoretical curve can also be evaluated. Figure 5 shows the experimental points for the hydrogen heat exchanger for the temperature of

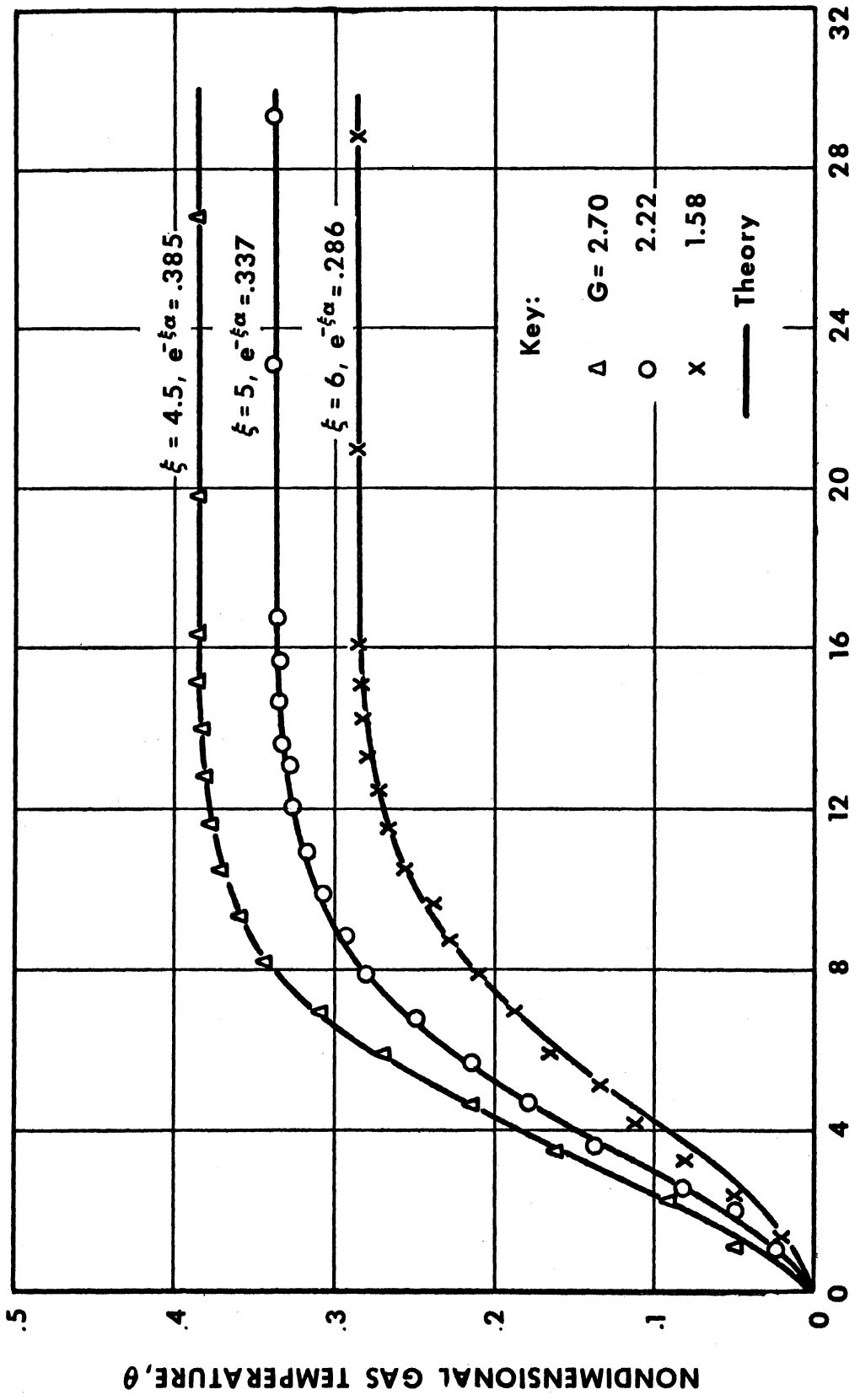

Fig. 5. θ vs. η for hydrogen heat exchanger.

the gas at a point 37 in. downstream from the inlet. The theoretical curves are shown in solid lines and one can see that the agreement is excellent for the three flows reported.

Unfortunately, because the air heat exchanger was not instrumented carefully to get heat-transfer data, no direct correlation between experimental points and theory was possible. However, the temperature of the gas at approximately one foot downstream from the end of the heat exchanger was measured for three different flows. The data are shown in Fig. 6 and it is evident that they show a trend which is expected from the theoretical analysis.

The experimental blowdown temperature of the air cannot be compared with the analytical solution of Refs. 4, 5, and 6. The reason is that these analyses are based on the assumption that the temperature of the bed material is uniform at the beginning of the blowdown period. It is known, however, that because of heat loss, the steady-state temperature in the bed material varies in an exponential manner[7] as shown in Fig. 7 for $t_o = 0$. In some cases, one can reasonably expect the temperature variation along the heat exchanger at later times, t_1, t_2, etc., to become as shown on the same figure. Thus when one plots the temperature at the exit of the heat exchanger, one can expect some rise and then an eventual drop. However, there will be a period during which the exit temperature remains relatively constant.

The experimental results did indicate a temperature increase and then a decrease as explained above. However, any testing where air at a constant temperature is required can be done during the period at which the temperature remains fairly constant. Figure 8 shows the exit temperature during such a period for the case where the flow rate was $G = 0.637$ lbm/sec-ft^2. It can be seen that three minutes after starting the flow the temperature remained fairly constant for four minutes which in this case was the duration of the test.

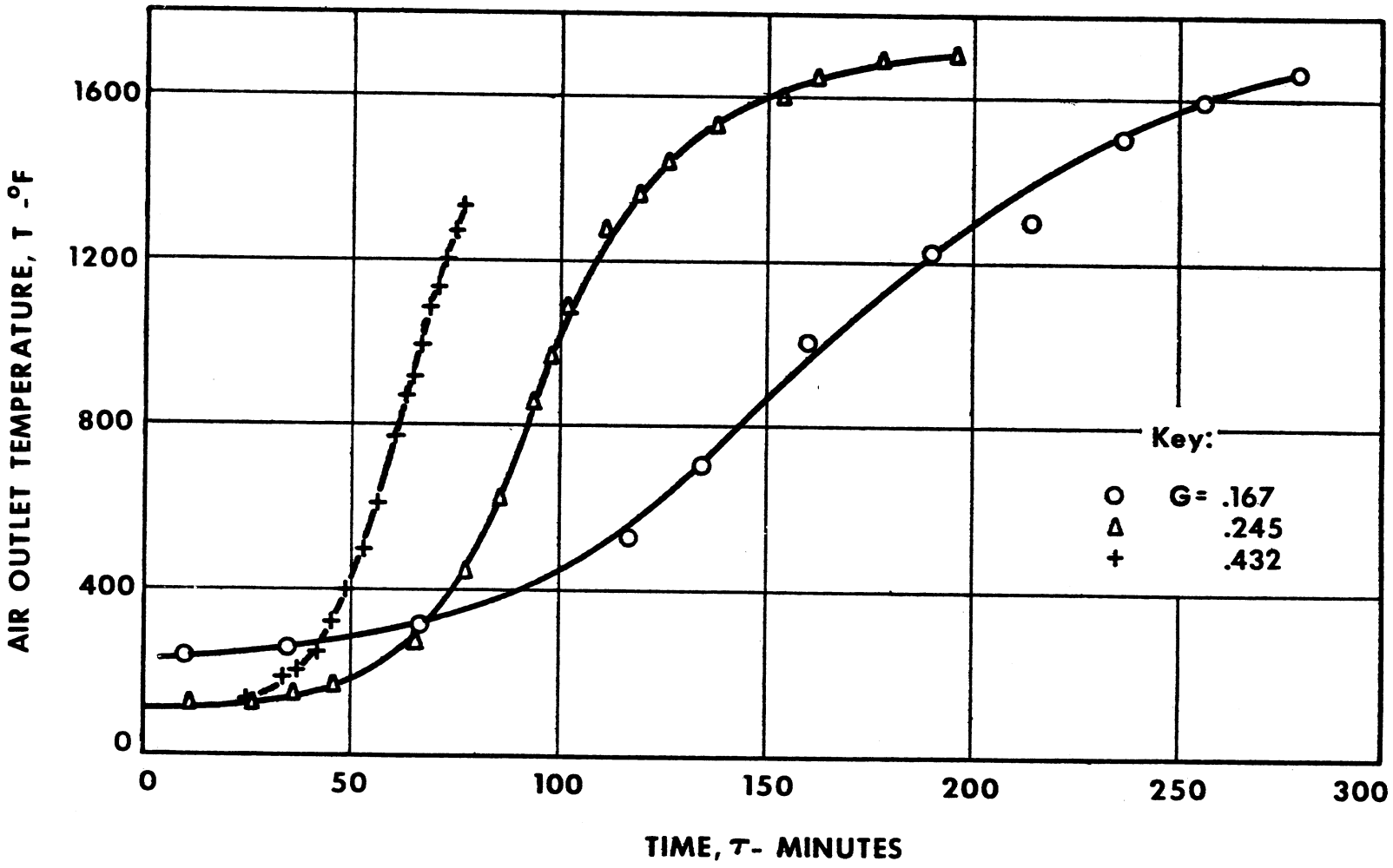

Fig. 6. Experimental T vs. τ for air heat exchanger.

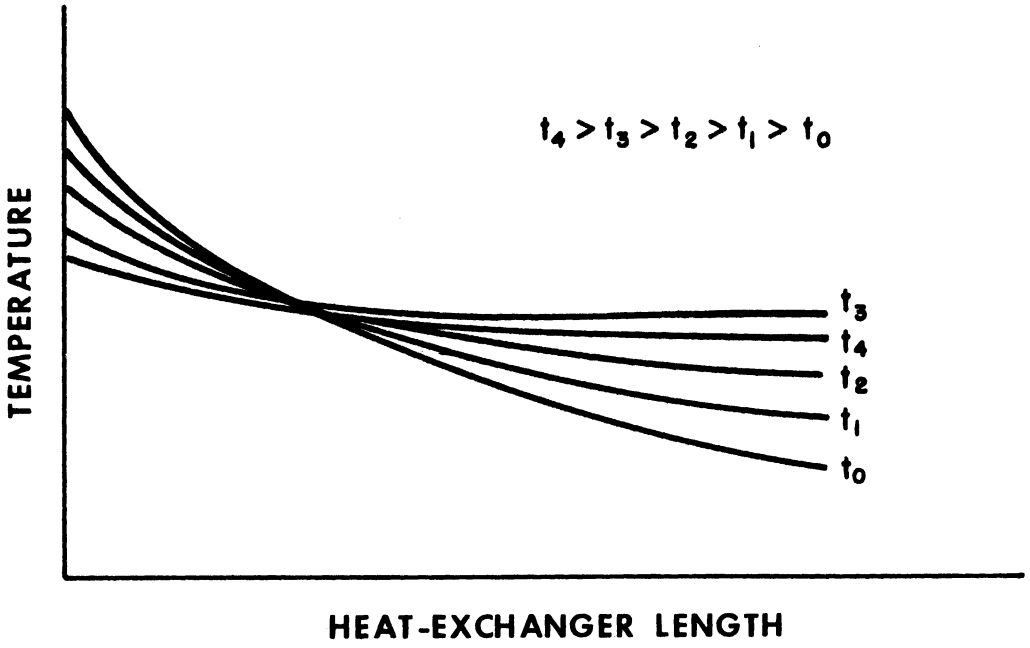

Fig. 7. Expected temperature variation during blowdown period.

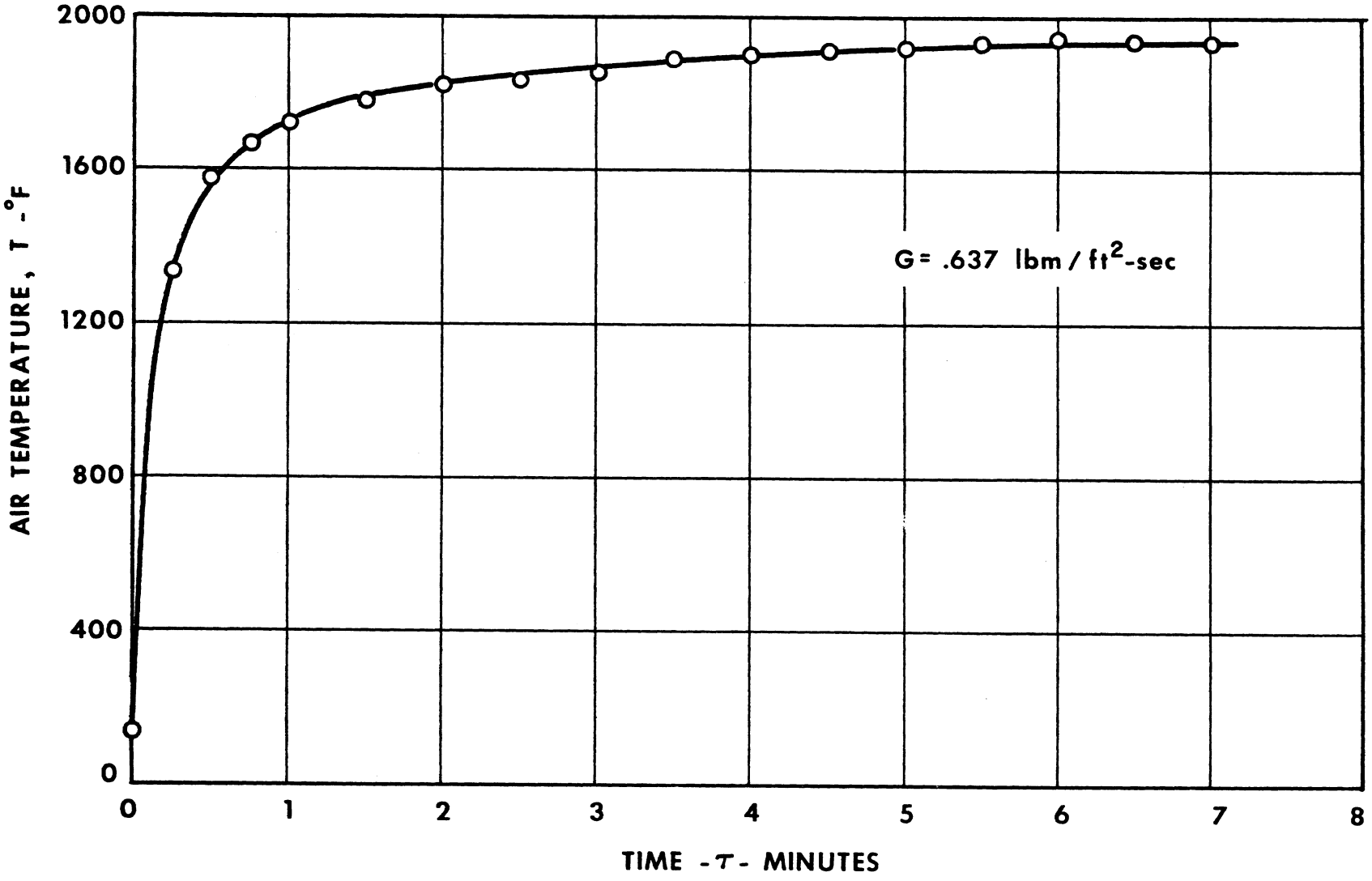

Fig. 8. Experimental T vs. τ for air heat exchanger during blowdown period.

IV. PRESSURE DROP

For the ranges of air flows in which we are interested, namely, 0.1 - 0.5 lbm/sec., the pressure drop across the air heat exchanger as calculated by a method similar to that described in Ref. 12 is negligible. For example, for a flow rate of .2 lbm/sec, the pressure drop is only 1.9 psi when one assumes the air pressure is nearly atmospheric and its temperature 1000°R. For the same flow and temperature conditions but with an average pressure of 750 psi, the pressure drop is estimated to be only 0.04 psi.

The pressure drop in the hydrogen heat exchanger for a flow rate of 0.0045 lbm/sec H_2 at average temperature and pressure of 1000°R and 800 psi, respectively, is calculated to be equal to 0.58 psi.

The above calculations are considered reliable since the friction factor as calculated from the pressure-drop data for compressed air using the hydrogen heat exchanger indicated very close agreement with friction-factor data reported in Ref. 12.

V. CORRELATION OF HEAT-TRANSFER DATA

Heat-transfer data for porous media are usually correlated by the use of dimensionless parameters such as the Reynolds, Nusselt, Stanton, and Prandtl numbers. Because of the difficulty of defining the heat-transfer surface in such media, a heat-transfer coefficient based on volume will be used as was done in Refs. 10 and 11. Also, to find the characteristic length necessary for evaluating the Reynolds and Nusselt numbers, use of a concept that apparently originated with Reynolds[10] is made: namely, that resistance to flow in a porous medium is made up of the superposition of viscous and inertial effects.

Thus, it is possible to write:

$$\frac{\Delta p}{x} = a\,\mu V + b\rho V^2 \quad . \tag{8}$$

The coefficients a and b can be determined from data of limited range when flow is isothermal by rewriting (8) as:

$$\rho \frac{\Delta p}{xG} = a\,\mu + bG \quad . \tag{9}$$

From friction data such as those given in Ref. 12, one can find a and b. Green[10] has shown that a very good approximation for $\ell = b/a$ can be obtained by the equation:

$$\ell = b/a = \frac{3.8 \times 10^{-2}}{s} \quad . \tag{10}$$

The latter equation is used in this report for the determination of the characteristic length.

The following table shows the calculated values necessary in the determination of St and Re using b/a as the characteristic length, the heat-exchanger length, x_1 = 37 in., and heat-exchanger overall cross-section area = 0.0167 ft^2 . The calculations are also based on air properties at an average temperature of 1300°F. The heat-storage medium is alumina pebbles 3/8-in. nominal size and .448-in. average diameter. The surface area per unit volume was taken as s = 104 ft^2/ft^3, which was computed by finding the number of pebbles per unit volume. From Eq. (10), ℓ is found to be 3.65×10^{-4} ft. By using friction data from Ref. 13, ℓ was found to be 4.35×10^{-4}, which agrees fairly well with the value obtained by Eq. (10).

w (lbm/sec)	G (lbm/ft^3-sec)	ξ	sh (Btu/ft^3-sec°F)	St	St $Pr^{2/3}$	Re
.0264	1.58	6	.832	7.1×10^{-4}	5.54	21.4
.0370	2.22	5	.974	5.94×10^{-4}	4.63	30.0
.0451	2.70	4.5	1.064	5.32×10^{-4}	4.15	36.5

The above data are shown in Fig. 9. In addition one point representing the best run on the air heat exchanger is included. On the same figure are lines showing the approximate correlation of the data of Ref. 13 on wire screens and lead spheres by Green[10] as well as the approximate correlation of Marco and Han[11] on steel wool. It is interesting to note that all three curves have practically the same slope. Thus the effect of the Reynolds number is the same in all three cases, indicating flow similarity.

VI. DISCUSSION OF RESULTS

Other literature surveyed[14,15,16,17] shows that most of the heat-transfer data would lie close to the upper curve of Fig. 9. This led some observers to believe that heat loss which was unaccounted for was the cause of the unusually low heat-transfer values obtained in Ref. 11. Although this may very likely be the case, it can hardly justify a difference of two orders of magnitude as Fig. 9 shows. Despite the fact that heat loss is taken into consideration in the calculation of the heat-transfer coefficient in this report, still lower values than those of Ref. 10 are obtained. This indicates the possibility that other parameters than have heretofore been entered into the correlation are important. One of these could be, for example, the ratio of the heat-exchanger diameter to the characteristic length of the heat-transfer medium.

Although no attempt is being made to make a full explanation of the lower values obtained here, it is perhaps enough to say that the heat-exchange medium used is acting as if the heat-transfer coefficient is lower than the correlation of Ref. 10 would indicate. In other words, most of the data reported in the literature on the subject do not give conservative enough values for design purposes.

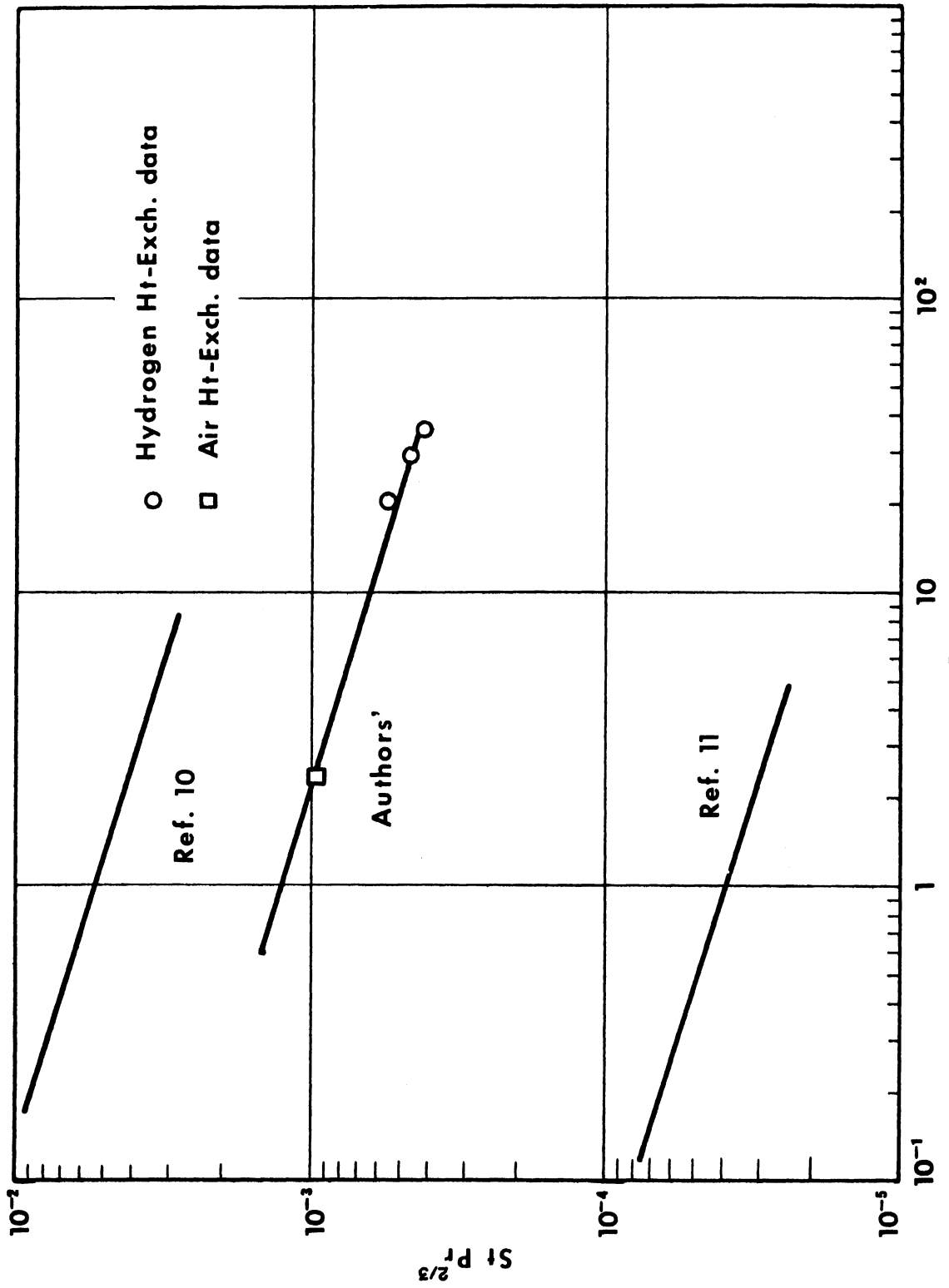

Fig. 9. St $Pr^{2/3}$ vs. Re.

In essence the reliability of the heat-transfer coefficients obtained experimentally depends upon the validity of the assumptions made in deriving the theoretical solution.

These assumptions are as follows:

1. The conductivity of the bed material is considered negligible in the direction of flow but very large in the direction transverse to the flow.
2. Heat transfer by conduction within the fluid is negligible.
3. The fluid is at uniform velocity across the bed.
4. End effects are negligible.
5. Heat loss to the surroundings occur in the radial direction.
6. The overall coefficient of heat transfer to the surroundings is constant.

The validity of assumption 1 can be seen when it is realized that there is very little surface contact between the individual pebbles so that little conduction is expected. However, because the pebbles are small, one would expect a uniform temperature at any section. This is the same as saying that conductivity is large in the radial direction.

Assumption 2 is valid when we are dealing with a gas of low thermal conductivity such as air. Assumption 3 is realized very shortly after entrance to the heat-transfer medium. The tortuous path of the fluid produces considerable mixing and therefore tends to create a uniform temperature and velocity distribution across the bed.

For assumption 4, the end effects are minimized by making the inlet to the pebble bed far from the exit to the burner and keeping the temperature of the gas at the inlet constant. The other end effect is avoided by taking temperature measurement well within the bed material.

Assumption 5 is rather weak, especially if the insulation is thick, for longitudinal conduction will then increase the loss. This, however, is taken care of by introducing the term "equivalent heat capacity" of the bed material which would include in addition a part of the heat capacity of the insulation mentioned on p.

Finally, assumption 6 can be considered reasonable enough only if the insulation resistance is controlling. This way the inside heat-transfer coefficient which would be changing with temperature has very little effect. Since the insulation was thick, this was the case with both the air and hydrogen heat exchangers.

In view of the above discussion, the results are considered valid.

VII. CONCLUSIONS

1. The effect of heat-loss parameter $\xi\alpha$ on the transient and steady-state temperature has been shown to agree with the theoretical analysis (see Fig. 5). For this reason, a careful evaluation of this product is essential for the purpose of predicting the steady-state temperature at the exit of a regenerative heat exchanger.

2. Heat-transfer coefficients evaluated from the experimental results are lower than those generally found in the literature despite the fact that heat loss has been accounted for. Although no explanation could be found, it is suggested that when values of heat-transfer coefficients as obtained from the literature are used, they should at least not be considered to yield a conservative design.

3. In evaluating the heat capacity of the bed material, allowance should be made to include at least part of the heat capacity of the insulation. What this part should be depends upon the expected temperature distribution in the insulation.

REFERENCES

1. Rutkowski, J., and Nicholls, J. A., "Considerations for Attainment of a Standing Detonation Wave," Proceedings of the Gas Dynamics Symposium, Northwestern University, 1956. Also issued as OSR-TN-55-216.

2. Liu, T. S., Sun, E. J. C. and Knutson, R. K., Construction of a Wind Tunnel Simulating the Aerodynamic Heating Effects on Aircraft Structures, WADC Technical Report 56-215, May, 1956.

3. Bloom, M. H., A High Temperature-Pressure Air Heater (Suitable for Intermittent Hypersonic Wind-Tunnel Operation), WADC Technical Note 56-694, ASTIA Doc. No. AD 110725, November, 1956.

4. Anzelius, A., "Über Erwärmung Vermittels Durchströmender Medien," Z.A.M.M., 6, 291 (1926).

5. Schumann, T. E. W., "Heat Transfer: A Liquid Flowing Through a Porous Prism," J. Franklin Institute, 208, 405-16 (1929).

6. Furnas, C. C., "Heat Transfer from a Gas to a Bed of Broken Solids," Trans. AIChE, 24, 142-86 (1930).

7. Dabora, E. K., Regenerative Heat Exchanger with Heat Loss Consideration, AFOSR TN 57-613, ASTIA No. 136 603, August, 1957.

8. Johnson, J. E., Regenerator Heat Exchangers for Gas Turbines, A.R.C.R. and M., No. 2630, 1952.

9. Locke, G. L., Heat Transfer and Flow Characteristics of Porous Solids, Tech. Rept. No. 10, Navy Contract N6-ONR-251, Task Order 6, Dept of Mech. Eng., Stanford Univ., Stanford, California.

10. Green, L., Jr., Heat, Mass and Momentum Transfer in Flow Through Porous Media, ASME paper No. 57-HT-19.

11. Marco, S. M., and Han, L. S., An Investigation of Convection Heat-Transfer in a Porous Medium, ASME paper No. 55-A-104.

12. Calculating Pressure Drop Through Packed Beds of Spheres and 1/4 Inch to 8 Mesh Granular Material, pamphlet, Aluminum Co. of America, Pittsburgh, Pa., August, 1956.

13. Coppage, J. E., Heat Transfer and Flow Friction Characteristics of Porous Media, Dept. of Mech. Eng., Tech. Rept. No. 16, Stanford University, Stanford, California, December, 1952.

REFERENCES (concluded)

14. Weisman, J., "Effect of Void Volume and Prandtl Modulus on Heat Transfer in Tube Banks and Packed Beds," AIChE, 1, 342-8, September, 1955.

15. Tang, Y. S., Duncan, J. M., and Schwyer, H. E., Heat and Momentum Transfer Between Spherical Particle and Air Stream, NACA Tech. Note 2867, March, 1953.

16. Gamson, B. W., "Heat and Mass Transfer in Fluid-Solid Systems," Chem. Eng. Prog., 47, 19 (1951).

17. Tong, L. S., and London, A. L., Heat Transfer and Flow Friction Characteristics of Woven Screen and Crossed-rod Matrices, ASME paper No. 56-A-124.

DISTRIBUTION LIST

Agency	Copy
Chief, Document Service Center Armed Services Technical Information Agency Arlington Hall Station Arlington 12, Virginia	10
Commander Western Development Division (ARDC) Post Office Box 262 Inglewood, California	1
Commander AF Office of Scientific Research Washington 25, D. C. Attn: SRDC	2
Director, Office for Advanced Studies AF Office of Scientific Research Box 2035 Pasadena 2, California	1
Commander, European Office Air Research and Development Command 60 Rue Cantersteen Brussels, Belgium	2
Commander Air Force Armament Center Eglin Air Force Base, Florida	1
Commander Arnold Engineering Development Center Tullahoma, Tennessee Attn: Library, P.O. Box 162	2
Commander AF Cambridge Research Center L. G. Hanscom Field Bedford, Massachusetts Attn: CRQST-2	1
Commander AF Flight Test Center Edwards Air Force Base Muroc, California	1
Commander AF Special Weapons Center Kirtland Air Force Base New Mexico	1
Commander Holloman Air Development Center Holloman Air Force Base Alamogordo, New Mexico	1
Commander Air Force Missile Test Center Patrick Air Force Base Cocoa, Florida	1
Commander Wright Air Development Center Wright-Patterson Air Force Base Ohio Attn: Power Plant Lab. Aeronautical Research Lab. Direct. of Weapons Systems Operations WCOSR-3	4
Commanding Officer Maxwell Air Force Base, Alabama Attn: Air University Library	1

DISTRIBUTION LIST (Continued)

Agency	Copy
Commander Air Materiel Command Wright-Patterson Air Force Base Ohio	1
Office of the Chief of Ordnance Department of the Army Washington 25, D. C. Attn: ORDTB	1
Director Ballistics Research Lab Aberdeen Proving Ground, Maryland	1
Commanding Officer Office of Ordnance Research Duke Station Durham, North Carolina	1
Commanding Officer Redstone Arsenal Huntsville, Alabama	1
Commanding Officer White Sands Proving Ground Las Cruces, New Mexico	1
Naval Supersonic Laboratory Massachusetts Institute of Technology Cambridge 39, Massachusetts	1
Chief of Naval Research Department of the Navy Washington 25, D. C.	1
Director U. S. Naval Research Laboratory Washington 25, D. C.	1
Chief, Bureau of Aeronautics Department of the Navy Washington 25, D. C.	1
Chief, Bureau of Ordnance Department of the Navy Washington 25, D. C.	1
Commander Naval Ordnance Laboratory White Oak Silver Spring, Maryland	1
Commander Naval Ordnance Test Station Inyokern China Lake, California	1
Director Aeronautical Research, NACA 1512 H Street, N. W. Washington 25, D. C.	1
Director Ames Aeronautical Laboratory NACA Langley Field, Virginia	1
Director Lewis Flight Propulsion Lab. NACA Cleveland Airport Cleveland, Ohio	1
National Bureau of Standards Washington 25, D. C.	1
Office of Technical Services Dept. of Commerce Washington 25, D. C.	1
U. S. Atomic Energy Commission Technical Information Service 1901 Constitution Avenue Washington 25, D. C.	1

DISTRIBUTION LIST (Concluded)

Agency	Copy
Bureau of Mines Department of the Interior Pittsburgh, Pennsylvania	1
Commander AF Office of Scientific Research Air Research and Development Command Washington 25, D. C. Attn: Library	3
Aerophysics Development Company P. O. Box 949 Santa Monica, California	1
Atlantic Research Corporation Alexandria, Virginia	1
University of California Berkley, California Attn: Dr. A. K. Oppenheim	1
Fairchild Engine Division of Fairchild Engine and Airplane Corp. Deer Park, Long Island, New York Attn: Dr. Robert Gross	1
Johns Hopkins University Baltimore 18, Maryland Attn: Dr. Hoelscher	1
University of Minnesota Minneapolis 14, Minnesota Attn: Dr. Chang	1
ARDE Associates 14 William Street Newark 2, New Jersey	1
Experiment Incorporated Richmond 2, Virginia	1
Arthur D. Little, Inc. 30 Memorial Drive Cambridge 42, Massachusetts	1
Harvard University 10 Divinity Avenue Cambridge 38, Massachusetts Attn: Dr. H. Emmons	1
Commander Wright Air Development Center Wright-Patterson Air Force Base Ohio Attn: WCRRC, Mr. Karl Scheller	1
The University of Michigan Engineering Research Institute Library Ann Arbor, Michigan	1